Insulin can regulate GLUT4 internalization by signaling to Rab5 and the motor protein dynein

Jie Huang*, Takeshi Imamura*, and Jerrold M. Olefsky*†‡

*Department of Medicine, Division of Endocrinology and Metabolism, University of California at San Diego, La Jolla, CA 92093-0673; and †San Diego Veterans Administration Medical Research Service and the Whittier Institute for Diabetes, 9894 Genesee Avenue, La Jolla, CA 92037

Edited by Donald F. Steiner, University of Chicago, Chicago, IL, and approved September 20, 2001 (received for review July 18, 2001)

Insulin stimulates glucose transport by promoting translocation of the insulin-sensitive glucose transporter isoform 4 (GLUT4) from an intracellular compartment to the cell surface. This movement is accomplished by stimulation of GLUT4 exocytosis as well as inhibition of endocytosis. However, the molecular mechanisms for these effects remain unclear. In this study, we found that the GTP-binding protein Rab5 physically associated with the motor protein dynein in immunoprecipitants from both untransfected cells and cells transfected with GFP-Rab5 constructs. Microinjection of anti-Rab5 or anti-dynein antibody into 3T3-L1 adipocytes increased the basal level of surface GLUT4, did not change the insulin-stimulated surface GLUT4 level, and inhibited GLUT4 internalization after the removal of insulin. Photoaffinity labeling of Rab5 with [γ-^{32}P]GTP-azidoanilide showed that insulin inhibited Rab5-GTP loading. By using microtubule-capture assays, we found that insulin also caused a significant decrease in the binding of dynein to microtubules. Furthermore, pretreatment of cells with the PI3-kinase inhibitor LY294002 inhibited the effects of insulin on both Rab5-GTP loading and dynein binding to microtubules. In conclusion, these data indicate that insulin signaling inhibits Rab5 activity and the interaction of dynein with microtubules in a PI3-kinase-dependent manner, and that these effects may inhibit the rate of GLUT4 internalization. As such, our results present a previously uncharacterized insulin-signaling pathway involving Rab5, the motor protein dynein, and the cytoskeleton to regulate directional GLUT4 movement, facilitating GLUT4 distribution to the cell surface.

Insulin activates glucose uptake in adipose tissue and muscle by stimulating translocation of the insulin-sensitive glucose transporter isoform 4 (GLUT4) from an intracellular compartment to the cell surface (1–3). In the basal state, GLUT4 is predominantly localized to intracellular membrane compartments, including the *trans*-Golgi network, the early endosomes, and other membranous elements in the cytoplasm (4–6). Upon insulin stimulation, GLUT4-containing vesicles are translocated rapidly from these compartments to the plasma membrane. After insulin is withdrawn, GLUT4 is internalized and returns to its intracellular localization (1–3). Insulin not only stimulates GLUT4 exocytosis, but also inhibits GLUT4 endocytosis (7–9). Although dynamin has been shown to participate in GLUT4 endocytosis (10–12), the exact mechanisms of GLUT4 internalization and how insulin inhibits GLUT4 endocytosis still are not clear.

Rab GTPases regulate vesicular-membrane trafficking in both the exocytic and the endocytic pathways. One member of this family, Rab5, is a key regulatory molecule directing vesicle transport and endosomal fusion in the early endocytic pathway (13). Localized to the plasma membrane in clathrin-coated vesicles (CCVs) and early endosomes, Rab5 plays a role in the formation and budding of CCVs, their subsequent fusion with early endosomes, and the homotypic fusion between early endosomes (14–17). Mutational studies have shown that Rab5-S34N, a mutant defective in GTP-binding, inhibited transferrin endocytosis displaying a dominant-negative effect, whereas Rab5-Q79L, a mutant with reduced GTPase activity, behaved as a constitutively active mutant stimulating endosome fusion (18, 19). Furthermore, Rab5 also is involved in regulating the interaction of endosomes with microtubule networks, which suggests a possible connection between Rab5 and microtubules (20). However, direct evidence regarding this connection and understanding of the molecular mechanisms by which Rab5 regulates directional vesicular movement are lacking.

In this study, we have examined the mechanisms of GLUT4 internalization in 3T3-L1 adipocytes. We show that the GTP-binding protein Rab5 physically associates with the motor protein dynein in immunoprecipitants. After insulin stimulation and subsequent hormone removal, microinjection of anti-Rab5 or anti-dynein antibody into 3T3-L1 adipocytes inhibits movement of GLUT4 from the cell surface back to its intracellular compartment. Further, we show that insulin inhibits Rab5-GTP loading and decreases binding of dynein to microtubules in a PI3-kinase-dependent manner. These findings indicate that insulin signaling inhibits Rab5 activity and the interaction of dynein with microtubules, retarding the inward movement of GLUT4.

Materials and Methods

Materials. The EGFP-tagged wild-type and mutant Rab5-cDNA constructs were kindly provided by Stephen Ferguson (The John P. Robarts Research Institute, London, Ontario, Canada). Rabbit polyclonal anti-GLUT4 antibody (F349) was kindly provided by Michael Mueckler (Washington University, St. Louis), and mouse monoclonal anti-GLUT4 antibody (1F8) was purchased from Biogenesis (Brentwood, NH). Monoclonal anti-Rab5 and -Rab4 antibodies were purchased from Transduction Laboratories (Lexington, KY). Monoclonal anti-dynein intermediate chain antibody was purchased from Chemicon. Polyclonal anti-Rab4, anti-Rab5a, anti-Rab5b, anti-β-tubulin, anti-dynein heavy chain antibodies, horseradish peroxidase-linked anti-mouse, and anti-rabbit antibodies were purchased from Santa Cruz Biotechnology. Sheep IgG and rhodamine-conjugated, FITC-conjugated anti-rabbit, anti-mouse, and anti-sheep IgG antibodies were obtained from Jackson ImmunoResearch. DMEM and FBS were purchased from Life Technologies (Grand Island, NY). LY294002, wortmannin, and PD98059 were purchased from Calbiochem. Tubulin and other reagents were purchased from Sigma.

This paper was submitted directly (Track II) to the PNAS office.

Abbreviations: GLUT4, glucose transporter isoform 4; GFP, green fluorescent protein; PI3-kinase, phosphatidylinositol 3-kinase; DIC, dynein intermediate chain.

‡To whom reprint requests should be addressed at: Department of Medicine (0673), University of California at San Diego, 9500 Gilman Drive, La Jolla, CA 92093-0673. E-mail: jolefsky@ucsd.edu.

The publication costs of this article were defrayed in part by page charge payment. This article must therefore be hereby marked "*advertisement*" in accordance with 18 U.S.C. §1734 solely to indicate this fact.

 www.pnas.org/cgi/doi/10.1073/pnas.241368698

Cell Treatment and Transient Transfection. 3T3-L1 cells were cultured and differentiated as described (21). For preparation of whole-cell lysates for immunoprecipitation and immunoblotting experiments, 3T3-L1 adipocytes were serum starved for 4–5 h in DMEM media containing 0.1% BSA. The cells were stimulated with 17 nM of insulin for 10 or 20 min at 37°C. Some cells were stimulated with 17 nM of insulin for 20 min; insulin then was washed out, followed by incubation in serum-free and insulin-free DMEM containing 0.1% BSA at 37°C for the indicated periods of time.

Differentiated 3T3-L1 adipocytes were transiently transfected with EGFP-tagged wild-type Rab5, mutant Rab5-S34N, or Rab5-Q79L DNA construct by electroporation, as described (22). Briefly, 100 μg of EGFP-tagged plasmid DNA purified by endotoxin-free purification kit (Qiagen, Chatsworth, CA) were transfected into 3T3-L1 adipocytes by electroporation at 0.33 kV and 960 microfarads (Gene Pulser, Bio-Rad). After electroporation, the cells were replated on collagen-coated tissue-culture dishes and incubated in DMEM containing 10% FBS at 37°C for 24–36 h before immunoprecipitation experiments.

Microinjection. Microinjection was performed by using a semiautomatic Eppendorf microinjection system. To study insulin-stimulated GLUT4 translocation, cells were incubated after microinjection in serum-free medium at 37°C for 3–4 h, followed by insulin stimulation at 1.7 nM for 20 min. For GLUT4 internalization study, the cells were serum starved for 4–5 h and stimulated with 1.7 nM of insulin for 20 min. Immediately after the washing out of insulin, cells were microinjected with control sheep IgG, monoclonal anti-Rab5, polyclonal anti-Rab4, or polyclonal anti-dynein heavy chain antibody within 10 min. The cells then were incubated in serum-free medium at 37°C for different periods of time, and fixed and processed for immunostaining as described below. All antibodies without any preservatives for microinjection were dissolved in microinjection buffer containing 5 mM sodium phosphate (pH 7.2) and 100 mM KCl.

Immunofluorescence Microscopy. Immunostaining and analysis of GLUT4 localization was performed as described (23–26). Briefly, cells were fixed with 3.7% (vol/vol) formaldehyde in PBS for 10 min at room temperature. After being permeabilized with 0.1% Triton X-100 for 10 min and blocked with 3% (vol/vol) FBS in PBS for 10 min, cells were incubated with anti-GLUT4 antibody (F349 or 1F8) in PBS with 3% (vol/vol) FBS overnight at 4°C, followed by incubation with rhodamine-conjugated secondary antibodies at room temperature for 1 h. Injected cells were detected with FITC-conjugated secondary antibodies. Cell-surface GLUT4 was analyzed by using immunofluorescence microscopy. The FITC-positive microinjected cells were evaluated for the presence of plasma membrane-associated GLUT4 staining. The cells displaying a fluorescence ring at the cell surface were scored positive. The percentage of positive cells was then used to represent the cell-surface GLUT4 level. The observer was blinded to the experimental condition of each coverslip.

Immunoprecipitation and Western Blotting. 3T3-L1 adipocytes were serum starved and stimulated with insulin as described above. The cells then were lysed in a solubilizing buffer containing 50 mM Hepes, 1 mM EDTA, 150 mM NaCl, 0.5% Nonidet P-40, 50 units per ml aprotinin, 1 mM Na_3VO_4, 1 mM PMSF, and 10 mM NaF (pH 7.4) for 20 min at 4°C. The soluble fractions were immunoprecipitated with antibodies at 4°C for 2 h, followed by incubating with protein A/G beads for 2 h. The immunoprecipitants were boiled in Laemmli sample buffer containing 100 mM DTT and resolved by SDS/PAGE. Gels were transferred to poly(vinylidene difluoride) membrane (Immobilon-P, Millipore) by using a Transblot apparatus (Bio-Rad). For immunoblotting, membranes were blocked and then probed with specific primary antibodies. After washing, blots were incubated with horseradish peroxidase-linked secondary antibodies followed by chemiluminescence detection (Pierce).

Microtubule Capture Assay. Microtubule capture assays were performed as described (27). Taxol-stabilized microtubules were prepared by incubating tubulin (Sigma) in 50 mM Pipes, pH 6.9/1 mM EGTA/0.5 mM $MgSO_4$/0.1 mM GTP with 20 μM taxol at 37°C for 30 min. 3T3-L1 adipocytes were serum-starved and stimulated with insulin as described above. Cells then were lysed in a lysis buffer containing BRB40 (40 mM Pipes, pH 6.9/1 mM EGTA/1 mM $MgCl_2$), 1% Triton X-100, 2 mM DTT, and protease inhibitors for 20 min at 4°C. The soluble fractions were incubated with monoclonal anti-dynein intermediate chain antibody and protein A Sepharose beads for 2 h at 4°C. After washing with cold BRB40 containing 10% (vol/vol) glycerol three times, the immunoprecipitants were incubated with 0.2 mg/ml taxol-stabilized microtubules/20 μM taxol/1 mM AMP-PNP for 30 min at 4°C. The beads then were washed with cold BRB40 five times, boiled in Laemmli sample buffer, and the amount of microtubules captured in the dynein immunoprecipitants was analyzed by SDS/PAGE and immunoblotting.

Photoaffinity Labeling of Rab5 with [γ-^{32}P]GTP-Azidoanilide. Serum-starved 3T3-L1 adipocytes were stimulated with 17 nM insulin for different periods of time. Whole-cell lysates (800 μg of protein) were incubated with 10 mM [γ-^{32}P]GTP-azidoanilide (Affinity Labeling Technologies, Lexington, KY; 12.2 mCi/μmol) for 1 min, and followed by UV-irradiation (254 nm) for 1 min on ice. Photoincorporation was stopped by the addition of 10 mM DTT. Samples then were immunoprecipitated with anti-Rab5 antibody at 4°C, and the immunoprecipitants were resolved by SDS/PAGE. Samples immunoprecipitated without primary antibody were used as negative controls. Gels were dried and signals were quantitated by a PhosphoImager (Molecular Dynamics).

Results and Discussion

Effect of Rab Proteins on GLUT4 Translocation. To assess the role of Rab5 in GLUT4 trafficking, we microinjected monoclonal anti-Rab5, rabbit anti-Rab4 antibody, or control sheep IgG into 3T3-L1 adipocytes, and measured GLUT4 at the plasma membrane by using immunofluorescence microscopy. Rab4 is involved in vesicular transport from endosomes to the plasma membrane and is important for resensitization of receptors (17, 28). As we reported (24), microinjection of Rab4 antibody inhibited insulin-induced GLUT4 translocation (Fig. 1*a*). Interestingly, in the absence of insulin, microinjection of Rab5 antibody increased the level of plasma membrane GLUT4 but did not change the insulin-stimulated surface-GLUT4 level (Fig. 1*a*). The increased cell-surface GLUT4 level in the Rab5 antibody-injected cells could be caused by either a decrease in the rate of the GLUT4 internalization or a delay in GLUT4 internalization, or both. To test specifically the effect of Rab4 and Rab5 on GLUT4 internalization, 3T3-L1 adipocytes were stimulated with 1.7 nM insulin for 20 min. The insulin then was rapidly removed by washing, and the cells then were microinjected with control IgG, anti-Rab5, or anti-Rab4 antibody. Compared with the IgG control, Rab4 antibody injection did not affect GLUT4 internalization as measured by the decrease in surface GLUT4 over time after insulin removal. However, Rab5 antibody injection led to an ≈50% inhibition of GLUT4 internalization after insulin withdrawal, as seen in Fig. 1*b*. The GLUT4 internalization rates observed in this study are quite comparable to the internalization rates published recently using

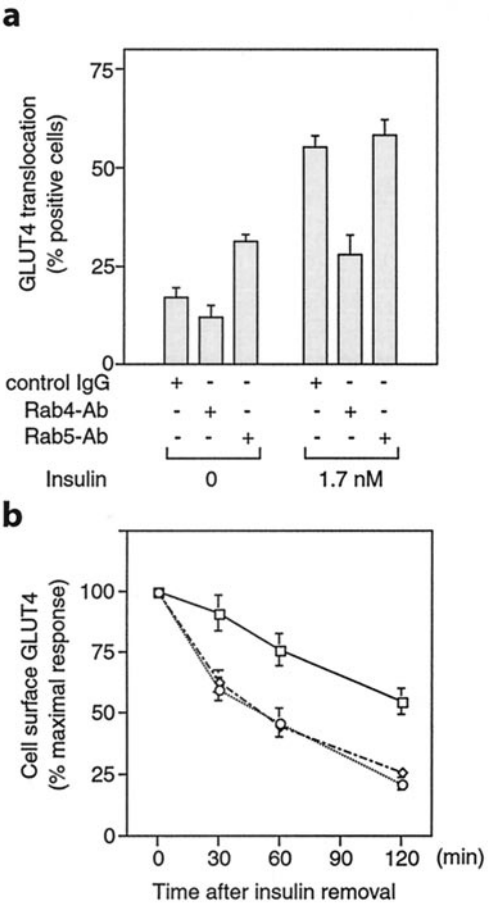

Fig. 1. Rab5 is involved in GLUT4 internalization in 3T3-L1 adipocytes. (*a*) Serum-starved 3T3-L1 adipocytes were microinjected with control IgG, anti-Rab4, or anti-Rab5 antibody, followed by stimulation with or without insulin for 20 min. GLUT4 translocation was scored by using immunofluorescence microscopy. (*b*) After 3T3-L1 cells were stimulated with insulin for 20 min, the insulin was washed out. The cells then were microinjected with control IgG (○), anti-Rab4 (◇), or anti-Rab5 antibody (□), followed by incubation in serum-free medium at 37°C for the indicated periods of time. Cell-surface GLUT4 was measured by using immunofluorescence microscopy. Data represent the mean ± SE of three experiments.

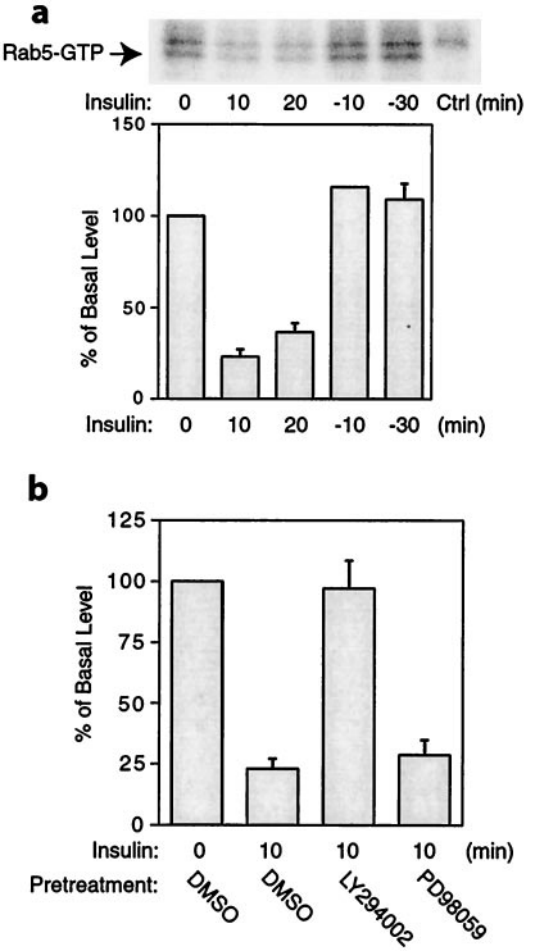

Fig. 2. Insulin inhibits Rab5-GTP loading. (*a*) Cells were treated with 17 nM insulin (0, 10, or 20 min). After insulin treatment for 20 min, insulin was removed by washing, and some of the cells were incubated in serum-free medium for 10 (-10) or 30 (-30) min. Cells were then lysed and photolabeled with [γ-^{32}P]GTP-azidoanilide. The samples were immunoprecipitated with anti-Rab5 antibody, and the immunoprecipitants were resolved by SDS/PAGE. Ctrl, negative control. (*b*) Cells were pretreated with 50 μM LY294002, 30 μM PD98059, or DMSO vehicle for 30 min, followed by insulin treatment for 10 min, and then photolabeled with Rab5 with [γ-^{32}P]GTP-azidoanilide, as described in *Materials and Methods*. Data were quantitated by a PhosphoImager, as represented in the bar graph. Data represent the mean ± SE of three experiments.

3T3-L1 adipocytes expressing a c-Myc–GLUT4–GFP construct (29). However, other reports have shown somewhat faster internalization rates (7, 30). These differences across studies may reflect the differences in cell types used (3T3-L1 adipocytes compared with L6 myocytes or primary adipocytes), or other aspects of the experimental conditions. In conclusion, our data indicate that Rab5 is involved in the process of GLUT4 internalization in 3T3-L1 adipocytes, which is consistent with other reports showing that Rab5 plays a critical role in regulating endocytic processes (13, 17–19).

Insulin Signaling Causes Inactivation of Rab5. Rab5 cycles between an active, GTP-bound form and an inactive, GDP-bound form. We investigated whether the activity of Rab5 changed in response to insulin. We treated cells with or without insulin and then immunoprecipitated the cell lysates with anti-Rab5 antibody and measured the Rab5-GTP level by using [γ-^{32}P]GTP-azidoanilide photoaffinity labeling. As shown in Fig. 2*a*, Rab5-GTP was readily detected in unstimulated 3T3-L1 cells. After insulin stimulation for 10 or 20 min, the Rab5-GTP level was reduced by 65–75% of the basal level. At 10 min after insulin was removed, Rab5-GTP had recovered to basal levels. These results indicate that Rab5 is activated in the basal state and is inactivated during the process of insulin-stimulated GLUT4 translocation, becoming reactivated when insulin's effects dissipate, allowing GLUT4 endocytosis to proceed normally. These results also are consistent with our microinjection data showing that Rab5 antibody injection increased the basal cell-surface GLUT4 level, did not change the insulin-stimulated surface GLUT4 level, and inhibited GLUT4 internalization after insulin withdrawal.

Next, we examined whether the effect of insulin on Rab5 was through a PI3-kinase sensitive pathway. We pretreated cells with the PI3-kinase inhibitor LY294002, the mitogen-activated protein kinase kinase (MEK) inhibitor PD98059, or DMSO vehicle for 30 min before insulin treatment for 10 min. We found that pretreatment with LY294002 blocked completely the inhibitory effect of insulin on Rab5, but PD98059 had no effect (Fig. 2*b*). These results suggest that Rab5 activity is regulated by insulin signaling through a PI3-kinase sensitive

pathway. As AKT/PKB is downstream of PI3-kinase (31), it is possible that AKT/PKB also may be involved in regulating Rab5 activity. It has been shown that an alternative pathway involving CAP, Cbl, C3G, and TC10 also is required for insulin-stimulated glucose transport, and that this pathway is independent of PI3-kinase (32, 33). Because our data showed that the effect of insulin on Rab5-GTP loading was PI3-kinase dependent, it seems unlikely that the CAP-Cbl pathway mediates the effects of insulin on Rab5-GTP loading. An insulin-induced change in Rab5 subcellular localization independent of PI3-kinase has been reported (34), suggesting that insulin-induced Rab5 movement and Rab5-GTP loading are differentially regulated. It has been shown that insulin inhibits the rate of GLUT4 endocytosis (7–9); however, the mechanism for this effect is unknown. Taken together, our data are consistent with the possibility that inactivation of Rab5 plays a role in the inhibition of GLUT4 internalization.

Interactions Between Rab5 and the Motor Protein Dynein. Microtubules play an important role in intracellular trafficking of vesicles and organization of organelles by providing the tracks on which motor proteins convey their cargoes (35). It has been reported that an intact microtubule cytoskeleton is required for perinuclear localization of GLUT4, insulin-stimulated GLUT4 translocation, and glucose uptake (36, 37). Cytoplasmic dynein, a multisubunit motor protein that moves along microtubules toward their minus ends, has been implicated to play a role in the perinuclear positioning of Golgi, lysosomes, GLUT4 vesicles, the assembly of mitotic spindles, and retrograde axonal transport (35, 38–40). A connection between Rab5 and microtubules has been suggested by the demonstration that, *in vitro*, Rab5 stimulated both association of endosomes with microtubules and minus-end motility of endosomes on microtubules (20). A kinesin-like protein, Rabkinesin-6, has been identified to interact with Rab6 (41), suggesting that motor proteins may be the connection between Rab GTPases and the cytoskeleton. Along these lines, we hypothesized that Rab5 regulated GLUT4 vesicle endocytosis through an association with the motor protein dynein. To test this hypothesis, we immunoprecipitated 3T3-L1 cell lysates with Rab5 or Rab4 antibody, and immunoblotted with anti-dynein intermediate chain (DIC) antibody. We found an association of Rab5 with dynein that was constant in basal, insulin stimulated, and insulin-withdrawn cells, but we found no association of Rab4 with dynein (Fig. 3*a*). To confirm this association of Rab5 with dynein, we also immunoprecipitated cell lysates with anti-DIC antibody and immunoblotted with Rab5 or Rab4 antibody; we found similar results (Fig. 3*b*). Furthermore, we transfected 3T3-L1 cells with GFP-tagged wild-type Rab5, dominant-negative Rab5 (S34N), and constitutively active Rab5 (Q79L), and immunoprecipitated the cell lysates with anti-GFP antibody. As shown in Fig. 3*c*, dynein was coprecipitated with all Rab5-GFP proteins, further confirming the association of Rab5 and dynein in 3T3-L1 cells. However, these coimmunoprecipitation experiments do not determine whether these interactions are direct or indirect through an intermediary molecule. Active Rab5 has been shown to interact with many different proteins (42). However, no association of Rab5 with a motor protein has yet been found. Thus, these results represent a demonstration of an association between Rab5 and a motor protein and raise the possibility that dynein is a functionally important Rab5 effector.

Effect of Insulin Signaling on Dynein Function. Cytoplasmic dynein has been found to remain on organelles during bidirectional transport, but its interaction with microtubules is regulated (27). We hypothesized that in 3T3-L1 cells, the association of dynein with microtubules was regulated by insulin signaling. To

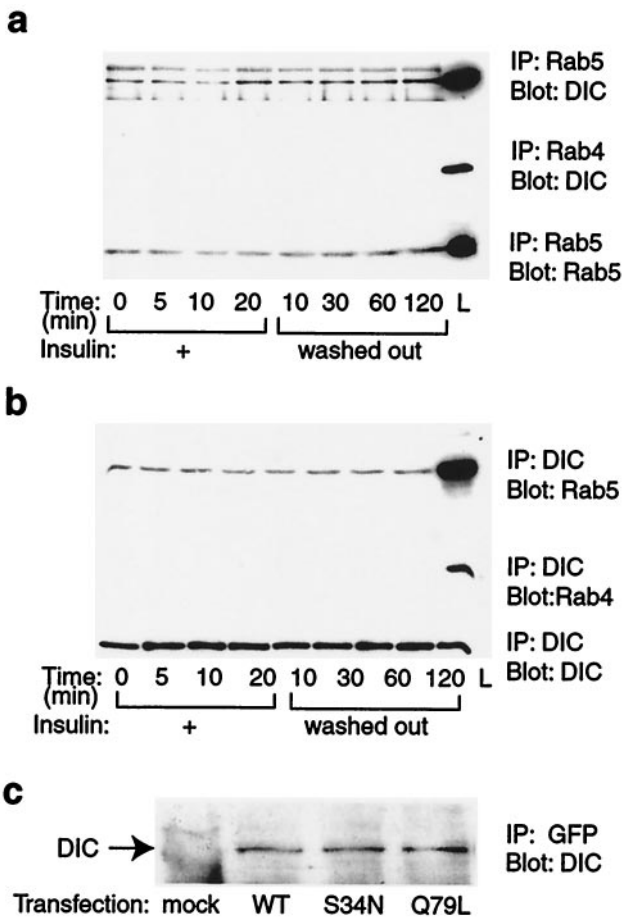

Fig. 3. Association of Rab5 with dynein in 3T3-L1 adipocytes. (*a*) Cells were treated with insulin for the indicated periods of time. Whole-cell lysates were immunoprecipitated with anti-Rab5 (*Top* and *Bottom*) or anti-Rab4 antibody (*Middle*) and immunoblotted with DIC (*Top* and *Middle*) or anti-Rab5 antibody (*Bottom*). L, whole-cell lysate. (*b*) Whole-cell lysates were immunoprecipitated with anti-DIC antibody and immunoblotted with anti-Rab5 (*Top*), anti-Rab4 (*Middle*), or anti-DIC antibody (*Bottom*). L, whole cell lysate. (*c*) 3T3-L1 cells were transfected with wild-type green fluorescent protein (GFP)-Rab5 (WT), dominant-negative mutant GFP-Rab5 (S34N), constitutively active GFP-Rab5 (Q79L) constructs, or mock control (mock). Transfected cell lysates were immunoprecipitated with anti-GFP antibody and immunoblotted with anti-DIC antibody. These experiments were repeated twice.

test this hypothesis, we performed microtubule-capture assays, in which immunoprecipitated dynein was incubated with taxol-stabilized microtubules. The amount of microtubule protein that remained associated with dynein after washing then was quantitated as a measure of dynein microtubule interaction. As shown in Fig. 4*a*, equal amounts of dynein were immunoprecipitated from unstimulated, insulin stimulated, and insulin withdrawn cells (Fig. 4*a Lower*); however, the amount of microtubules captured in dynein immunoprecipitants from insulin-stimulated cells was markedly reduced compared with unstimulated cells. At 10 or 30 min after insulin was removed, the amount of microtubules captured in dynein immunoprecipitants returned to the same values as seen in unstimulated cells (Fig. 4*a Upper*). These results suggest that, in the basal state, dynein binds to microtubules. Insulin stimulation leads to dissociation of dynein from microtubules, and after insulin removal, the two components reassociate. Next, we examined whether the effect of insulin on dynein binding to microtubules was mediated through a PI3-kinase sensitive pathway. We

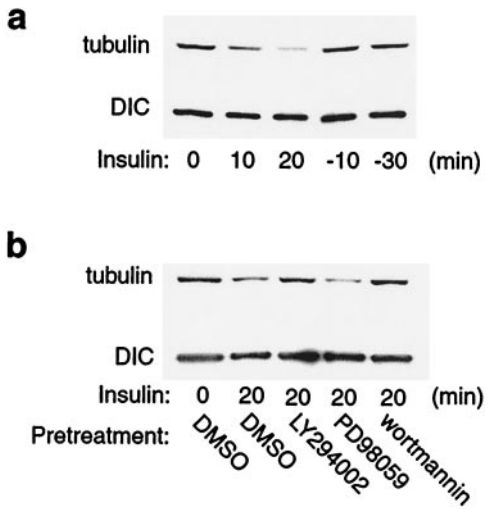

Fig. 4. Insulin stimulation causes dissociation of dynein from microtubules. (*a*) 3T3-L1 cells were treated with 17 nM insulin (0, 10, or 20 min). After insulin treatment for 20 min, insulin was removed by washing, and some of the cells were incubated in serum-free medium for 10 (-10) or 30 (-30) min. Whole-cell lysates were immunoprecipitated with anti-DIC antibody and processed for microtubule-capture assays. Tubulin was detected by immunoblotting with polyclonal anti-β-tubulin antibody. (*b*) Cells were pretreated with 50 μM LY294002, 30 μM PD98059, 100 nM wortmannin, or DMSO vehicle for 30 min, followed by insulin treatment for 20 min. Whole-cell lysates then were immunoprecipitated with anti-DIC antibody and processed for microtubule-capture assays. Taxol-stabilized microtubules were added to the dynein immunoprecipitants, and after extensive washing, the amount of tubulin bound was detected by SDS/PAGE and immunoblotted with polyclonal anti-β-tubulin antibody. These experiments were repeated twice.

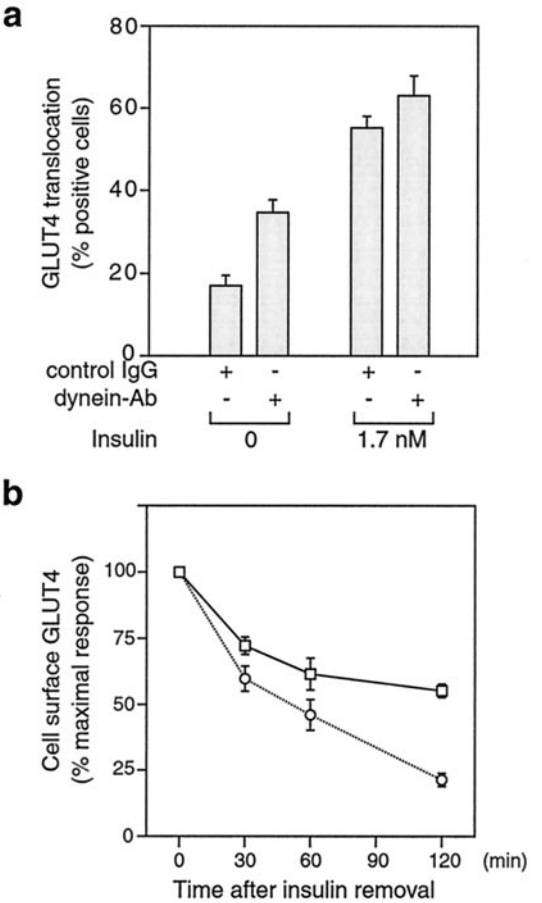

Fig. 5. Dynein is involved in minus end-directed GLUT4-vesicle transport in 3T3-L1 adipocytes. (*a*) Serum-starved 3T3-L1 adipocytes were microinjected with control IgG or rabbit polyclonal anti-dynein antibody, followed by stimulation with or without insulin for 20 min. GLUT4 translocation was scored by using immunofluorescence microscopy. (*b*) After 3T3-L1 cells were stimulated with insulin for 20 min, the insulin was removed by washing. The cells then were microinjected with control IgG (○) or rabbit polyclonal anti-dynein antibody (□), followed by incubation in serum-free medium at 37°C for the indicated periods of time. Cell-surface GLUT4 was measured by using immunofluorescence microscopy. Data represent the mean ± SE of three experiments.

pretreated cells with the PI3-kinase inhibitor LY294002 or wortmannin, the MEK inhibitor PD98059, or DMSO vehicle for 30 min, followed by insulin treatment for 20 min before the microtubule-capture assay. We found that pretreatment with LY294002 or wortmannin significantly inhibited the effect of insulin to decrease dynein microtubule binding, whereas PD98059 had no effect (Fig. 4*b*).

Microinjection of Dynein Antibody Inhibits GLUT4 Internalization. Finally, we investigated whether dynein was involved in GLUT4 vesicle trafficking in 3T3-L1 adipocytes. The cytoplasmic dynein heavy chain contains the ATPase and the motor domains (40). Similar to the effect of Rab5 antibody injection (Fig. 1), anti-dynein heavy chain antibody injection increased the basal level of GLUT4 at the cell surface, did not change the insulin-stimulated surface GLUT4 level (Fig. 5*a*), and inhibited GLUT4 internalization after insulin withdrawal (Fig. 5*b*). These results suggest that cytoplasmic dynein is involved in minus end-directed GLUT4 transport in 3T3-L1 adipocytes, indicating that dynein may play an important role in directing or targeting GLUT4 vesicles to the minus end of microtubules in 3T3-L1 cells that are located in the perinuclear region. Such an effect would serve to maintain the perinuclear localization of GLUT4 in the basal state. Indeed, studies from Guilherme *et al.* (36) have indicated that acidification of 3T3-L1 cells, which can disrupt dynein function, leads to the dispersion of GLUT4 vesicles from their basal perinuclear localization. The insulin-induced inactivation of Rab5 and dissociation of dynein from microtubules then would facilitate movement of GLUT4 vesicles to the cell surface and inhibit their subsequent endocytic return to the intracellular compartment. This concept also would explain why insulin-induced GLUT4 translocation is not augmented by injection of anti-Rab5 or dynein antibody, because the activity of both molecules is already inhibited by insulin, and further inactivation caused by antibody microinjection should have no added effect.

The literature already contains several suggestions indicating a potential role for Rab proteins in GLUT4 translocation (24, 43, 44). Furthermore, it is also known that an intact cytoskeleton is necessary for the movement of GLUT4 protein to the cell surface (36). The current paper provides evidence for a signaling mechanism linking these components, and demonstrates that this pathway is under the regulation of insulin in a way consistent with the process of insulin-stimulated GLUT4 translocation. Thus, Rab5 physically associates with the motor protein dynein, and insulin leads to deactivation of Rab5 and causes the dissociation of dynein from microtubules. When Rab5 is active and dynein binds to microtubules, this process would serve to facilitate internalization and localize GLUT4 vesicles to the perinuclear region of the cell. After insulin stimulation, the decreased activity of Rab5 and dissociation of dynein from microtubules would foster the release of GLUT4 vesicles to allow exocytosis to the cell surface. The consequent inhibition of GLUT4 inter-

nalization would enhance accumulation of glucose transporters at the cell surface, further augmenting glucose transport. Taken together, our data provide evidence for a previously uncharacterized action of insulin to mediate glucose transport stimulation. This new aspect of insulin action provides a molecular mechanism to explain the effect of insulin to inhibit the process of GLUT4 internalization, and contributes to a coordinated system facilitating insulin-stimulated movement of GLUT4 vesicles to the cell surface.

We thank Dr. Stephen Ferguson for kindly providing the wild-type and mutant EGFP-Rab5 DNA constructs. This work was supported by National Institutes of Health Grant DK33651 (to J.M.O.) and the American Diabetes Association Mentor-Based Postdoctoral Fellowship Award (to J.M.O.).

1. Olefsky, J. M. (1999) *J. Biol. Chem.* **274,** 1863.
2. Czech, M. P. & Corvera, S. (1999) *J. Biol. Chem.* **274,** 1865–1868.
3. Pessin, J. E., Thurmond, D. C., Elmendorf, J. S., Coker, K. J. & Okada, S. (1999) *J. Biol. Chem.* **274,** 2593–2596.
4. Slot, J. W., Geuze, H. J., Gigengack, S., James, D. E. & Lienhard, G. E. (1991) *Proc. Natl. Acad. Sci. USA* **88,** 7815–7819.
5. Slot, J. W., Geuze, H. J., Gigengack, S., Lienhard, G. E. & James, D. E. (1991) *J. Cell Biol.* **113,** 123–135.
6. Ploug, T., van Deurs, B., Ai, H., Cushman, S. W. & Ralston, E. (1998) *J. Cell Biol.* **142,** 1429–1446.
7. Jhun, B. H., Rampal, A. L., Liu, H., Lachaal, M. & Jung, C. Y. (1992) *J. Biol. Chem.* **267,** 17710–17715.
8. Yang, J. & Holman, G. D. (1993) *J. Biol. Chem.* **268,** 4600–4603.
9. Czech, M. P. & Buxton, J. M. (1993) *J. Biol. Chem.* **268,** 9187–9190.
10. Al-Hasani, H., Hinck, C. S. & Cushman, S. W. (1998) *J. Biol. Chem.* **273,** 17504–17510.
11. Kao, A. W., Ceresa, B. P., Santeler, S. R. & Pessin, J. E. (1998) *J. Biol. Chem.* **273,** 25450–25457.
12. Volchuk, A., Narine, S., Foster, L. J., Grabs, D., De Camilli, P. & Klip, A. (1998) *J. Biol. Chem.* **273,** 8169–8176.
13. Bucci, C., Parton, R. G., Mather, I. H., Stunnenberg, H., Simons, K., Hoflack, B. & Zerial, M. (1992) *Cell* **70,** 715–728.
14. Bucci, C., Lütcke, A., Steele-Mortimer, O., Olkkonen, V. M., Dupree, P., Chiariello, M., Bruni, C. B., Simons, K. & Zerial, M. (1995) *FEBS Lett.* **366,** 65–71.
15. McLauchlan, H., Newell, J., Morrice, N., Osborne, A., West, M. & Smythe, E. (1998) *Curr. Biol.* **8,** 34–45.
16. Rubino, M., Miaczynska, M., Lippé, R. & Zerial, M. (2000) *J. Biol. Chem.* **275,** 3745–3748.
17. Seachrist, J. L., Anborgh, P. H. & Ferguson, S. S. G. (2000) *J. Biol. Chem.* **275,** 27221–27228.
18. Stenmark, H., Parton, R. G., Steele-Mortimer, O., Lütcke, A., Gruenberg, J. & Zerial, M. (1994) *EMBO J.* **13,** 1287–1296.
19. Barbieri, M. A., Li, G., Mayorga, L. S. & Stahl, P. D. (1996) *Arch. Biochem. Biophys.* **326,** 64–72.
20. Nielsen, E., Severin, F., Backer, J. M., Hyman, A. A. & Zerial, M. (1999) *Nat. Cell Biol.* **1,** 376–382.
21. Imamura, T., Vollenweider, P., Egawa, K., Clodi, M., Ishibashi, K., Nakashima, N., Ugi, S., Adams, J. W., Brown, J. H. & Olefsky, J. M. (1999) *Mol. Cell. Biol.* **19,** 6765–6774.
22. Thurmond, D. C., Ceresa, B. P., Okada, S., Elmendorf, J. S., Coker, K. & Pessin, J. E. (1998) *J. Biol. Chem.* **273,** 33876–33883.
23. Morris, A. J., Martin, S. S., Haruta, T., Nelson, J. G., Vollenweider, P., Gustafson, T. A., Mueckler, M., Rose, D. W. & Olefsky, J. M. (1996) *Proc. Natl. Acad. Sci. USA* **93,** 8401–8406.
24. Vollenweider, P., Martin, S. S., Haruta, T., Morris, A. J., Nelson, J. G., Cormont, M., Le Marchand-Brustel, Y., Rose, D. W. & Olefsky, J. M. (1997) *Endocrinology* **138,** 4941–4949.
25. Imamura, T., Ishibashi, K., Dalle, S., Ugi, S. & Olefsky, J. M. (1999) *J. Biol. Chem.* **274,** 33691–33695.
26. Imamura, T., Huang, J., Dalle, S., Ugi, S., Usui, I., Luttrell, L. M., Miller, W. E., Lefkowitz, R. J. & Olefsky, J. M. (2001) *J. Biol. Chem.*, in press.
27. Reese, E. L. & Haimo, L. T. (2000) *J. Cell Biol.* **151,** 155–165.
28. van der Sluijs, P., Hull, M., Webster, P., Mâle, P., Goud, B. & Mellman, I. (1992) *Cell* **70,** 729–740.
29. Bogan, J. S., McKee, A. E. & Lodish, H. F. (2001) *Mol. Cell. Biol.* **21,** 4785–4806.
30. Li, D. L., Randhawa, V. K., Patel, N., Hayashi, M. & Klip, A. (2001) *J. Biol. Chem.* **276,** 22883–22891.
31. Corvera, S. & Czech, M. P. (1998) *Trends Cell Biol.* **8,** 442–446.
32. Baumann, C. A., Ribon, V., Kanzaki, M., Thurmond, D. C., Mora, S., Shigematsu, S., Bickel, P. E., Pessin, J. E. & Saltiel, A. R. (2000) *Nature (London)* **407,** 202–207.
33. Chiang, S. H., Baumann, C. A., Kanzaki, M., Thurmond, D. C., Watson, R. T., Neudauer, C. L., Macara, I. G., Pessin, J. E. & Saltiel, A. R. (2001) *Nature (London)* **410,** 944–948.
34. Cormont, M., Van Obberghen, E., Zerial, M. & Le Marchand-Brustel, Y. (1996) *Endocrinology* **137,** 3408–3415.
35. Hirokawa, N. (1998) *Science* **279,** 519–526.
36. Guilherme, A., Emoto, M., Buxton, J. M., Bose, S., Sabini, R., Theurkauf, W. E., Leszyk, J. & Czech, M. P. (2000) *J. Biol. Chem.* **275,** 38151–38159.
37. Fletcher, L. M., Welsh, G. I., Oatey, P. B. & Tavare, J. M. (2000) *Biochem. J.* **352,** 267–276.
38. Vallee, R. B. & Sheetz, M. P. (1996) *Science* **271,** 1539–1544.
39. Susalka, S. J., Hancock, W. O. & Pfister, K. K. (2000) *Biochim. Biophys. Acta* **1496,** 76–88.
40. King, S. M. (2000) *Biochim. Biophys. Acta* **1496,** 60–75.
41. Echard, A., Jollivet, F., Martinez, O., Lacapère, J. J., Rousselet, A., Janoueix-Lerosey, I. & Goud, B. (1998) *Science* **279,** 580–585.
42. Christoforidis, S., McBride, H. M., Burgoyne, R. D. & Zerial, M. (1999) *Nature (London)* **397,** 621–625.
43. Cormont, M., Gautier, N., Ilc, K. & Le Marchand-Brustel, Y. (2001) *Biochem. J.* **356,** 143–149.
44. Knight, J. B., Cao, K. T., Gibson, G. V. & Olson, A. L. (2000) *Endocrinology* **141,** 208–218.